Micheliolide suppresses the viability, migration and invasion of U251MG cells via the NF-κB signaling pathway

DINGKUN FENG[1], MIN LIU[2], YANTING LIU[3,4], XIAOJIN ZHAO[5], HUAN SUN[1], XU ZHENG[1], JIABIN ZHU[1,4] and FAJUN SHANG[1]

[1]Department of Neurosurgery, The Affiliated Renhe Hospital, China Three Gorges University, Yichang, Hubei 443000; [2]Department of Neurology, Xinhua Hospital affiliated to Dalian University, Dalian, Liaoning 116021; [3]Department of Neurosurgery; [4]Central Laboratory, The First College of Clinical Medical Science, China Three Gorges University & Yichang Central People's Hospital, Yichang, Hubei 443003; [5]Department of Gastroenterology, The Affiliated Renhe Hospital, China Three Gorges University, Yichang, Hubei 443000, P.R. China

Received December 21, 2019; Accepted June 16, 2020

DOI: 10.3892/ol.2020.11928

Abstract. Micheliolide (MCL), a sesquiterpene lactone isolated from *Michelia compressa* and *Michelia champaca*, has been used previously to inhibit the NF-κB signaling pathway. MCL has exerted various therapeutic effects in numerous types of disease, such as inflammatory and cancer. However, to the best of our knowledge, its underlying anticancer mechanism remains to be understood. The present study aimed to investigate the effects of MCL on human glioma U251MG cells and to determine the potential anticancer mechanism of action of MCL. From Cell Counting Kit-8, colony formation assay, apoptosis assay and Confocal immunofluorescence imaging analysis, the results revealed that MCL significantly inhibited cell viability *in vitro* and induced cell apoptosis via activation of the cytochrome *c*/caspase-dependent apoptotic pathway. In addition, MCL also suppressed cell invasion and metastasis via the wound healing and Transwell invasion assays. Furthermore, western blot and reverse transcription PCR analyses demonstrated that MCL significantly downregulated cyclooxygenase-2 (COX-2) expression levels, which may have partially occurred through the inactivation of the NF-κB signaling pathway. In conclusion, the results of the present study indicated that MCL may inhibit glioma carcinoma growth by downregulating the NF-κB/COX-2 signaling pathway, which suggested that MCL may be a novel and alternative antitumor agent for the treatment of human glioma carcinoma.

Correspondence to: Mr. Fajun Shang or Mr. Jiabin Zhu, Department of Neurosurgery, The Affiliated Renhe Hospital, China Three Gorges University, 410 Yiling Avenue, Yichang, Hubei 443000, P.R. China
E-mail: shangfajun01@sina.com
E-mail: zhujiabin@ctgu.edu.cn

Key words: micheliolide, glioma, cyclooxygenase-2, NF-κB

Introduction

Gliomas, which arise from transformed glial cells, are the most common, lethal type of primary tumor in the central nervous system, accounting for 60-70% of primary brain tumors and 80% of all malignant brain tumors (1,2). Previous studies have reported that glioma has an annual incidence of ~6/100,000 cases worldwide, with a high recurrence rate due to its diffuse invasive characteristics and malignant behavior, which results in a poor prognosis (3-5). Although neurosurgery combined with radio- and chemotherapy has contributed to considerable progress in the treatment of the glioma, the median survival time for patients with glioma remains at 12-15 months (6,7). Hence, there remains an urgent requirement to identify novel treatment strategies and effective therapeutic agents to extend and improve the survival and quality of life of patients.

Increasing evidence has established that chronic inflammation influenced almost every aspect of cancer progression (8-10) and increased the risk of cancer (11,12), such as the case with meningitis-associated malignant brain tumors (13). Inflammatory cells and molecules exist in the tumor microenvironment, which promote tumor development and progression, such as tumor growth, cell metastasis and even inflammation (14,15). Cyclooxygenase-2 (COX-2), one of the pivotal factors in the progress of inflammation, has been causally associated with the progression of numerous types of human tumor, including gliomas, lung cancer and breast cancer (9,16,17). In addition, COX-2 was discovered to be highly expressed in patients with glioma or glioma specimens (18), and was associated with the degree of tumor invasiveness and the prognosis of patients (19,20). Hence, the suppression of COX-2 expression with specific small molecule inhibitors may represent a potential therapeutic approach for the suppression of glioma development.

In the past few years, researchers have paid increasing attention to traditional Chinese medicines, due to their demonstrated potential to treat various types of cancer with low toxicity, such as lung cancer, breast cancer and glioma (9,17,21). Micheliolide (MCL) is a sesquiterpene lactone isolated from

Michelia compressa and *Michelia champaca* (22). Previous studies have demonstrated that MCL exerted various therapeutic effects in cancer, inflammation, immunomodulatory acute myelogenous leukemia and renal fibrosis (22-26) through numerous signaling pathways, including PI3K/Akt, NF-kB and MAPK signaling. Dimethylaminomicheliolide (DMAMCL), the prodrug of MCL, has been approved by the US Food and Drug Administration for its apparent efficacy in the treatment of pleomorphic glioblastoma (27,28). In China, DMAMCL is currently undergoing clinical trials for the treatment of several advanced or metastatic solid carcinomas, including gliomas (29). However, as an active molecule of DMAMCL, the therapeutic potential of MCL in gliomas and its underlying mechanisms remain unknown.

The findings of the present study suggested that MCL may potentially exert therapeutic effects against human glioma through promoting cell apoptosis and suppressing the NF-κB/COX-2 signaling pathway. Thus, the present study highlighted the novel roles of MCL in the treatment of human gliomas.

Materials and methods

Chemicals and reagents. MCL was purchased from Sigma-Aldrich; Merck KGaA. Temozolomide (TMZ) was purchased from Sigma-Aldrich; Merck KGaA. MCL stock solution was dissolved in DMSO and stored at -20˚C. Prior to use, the stock solution was diluted with DMEM medium (Gibco; Thermo Fisher Scientific, Inc.), and the final concentration of DMSO was adjusted to <0.1%. The control group was treated with carrier solvent (0.1% DMSO).

Antibodies and other materials. The following primary antibodies were purchased from Cell Signaling Technology, Inc.: Anti-cleaved caspase-3 (cat. no. 9664), anti-cleaved caspase-9 (cat. no. 7237), anti-COX-2 (cat. no. 12282), anti-phosphorylated (p)-IκBα (cat. no. 2859), anti-IκBα (cat. no. 9242) and anti-β-actin (cat. no. 3700). Anti-rabbit IgG, HRP-linked antibody (cat. no. 7074; 1:5,000) and anti-mouse IgG, HRP-linked Antibody cat. no. 7076; 1:5,000) secondary antibodies were also purchased from Cell Signaling Technology, Inc. The following primary antibodies were purchased from ProteinTech Group, Inc.: Anti-cytochrome *c* (cat. no. 66264-1-Ig), anti-Bcl-2 (cat. no. 12789-1-AP), anti-Bax (cat. no. 50599-2-Ig), anti-Vimentin (cat. no. 10366-1-AP), anti-matrix metalloproteinase (MMP)-9 (cat. no. 10375-2-AP) and anti-N-cadherin (cat. no. 22018-1-AP). DMEM, FBS and trypsin were purchased from Gibco; Thermo Fisher Scientific, Inc. Other chemicals (such as NaCl and KCl) were obtained from Sigma-Aldrich; Merck KGaA.

Cell culture. The human glioma cell line U251MG was obtained from the American Type Culture Collection. U251MG cells were cultured in DMEM, supplemented with 10% FBS, 100 U/ml penicillin and 100 μg/ml streptomycin, and maintained at 37˚C in a humidified atmosphere with 5% CO_2. The authenticity of U251MG cells was verified via genomic short tandem repeat profiling by Shanghai Zhongqiao Xizhou Biotechnology Co., Ltd., and the cells were confirmed to be free of mycoplasma using a Mycoplasma Detection kit (cat. no. MB000-1591) with UDG PCR Mix and Loading Dye (Excell Biotech, http://www.excellbio.com/productcenter/info.aspx?itemid=274&Lcid=42).

Cell viability assay. Briefly, $6x10^3$ U251MG cells/well were seeded into 96-well plates in 100 μl media. Cells were allowed to adhere overnight and then treated with different concentrations of MCL (0, 2.5, 5, 10 or 20 μM) for 24 and 48 h at 37˚C. Subsequently, 10 μl Cell Counting Kit-8 (CCK-8) buffer (Dojindo Molecular Laboratories, Inc.) was added into each well and incubated for 1.5 h at 37˚C according to the manufacturer's protocol. The absorbance at a wavelength of 450 nm was measured using a microplate reader (PerkinElmer, Inc.).

Colony formation assay. U251MG cells were incubated with 0, 5, 10 or 15 μM MCL for 24 h at 37˚C and then digested into single cells by trypsinization. U251MG cells were seeded into 6-well plates at a density of $1.5x10^3$ cells/well. Following incubation for 14 days at 37˚C with 5% CO_2, the colonies were washed with PBS and fixed with the mixture buffer (methanol: glacial acetic acid, ddH_2O=1:1:8) for 10 min at room temperature, then stained with 0.1% crystal violet for 30 min at room temperature. The number of colonies (diameter >1 mm) were counted using an EVOS XL Core inverted light microscope inverted light microscope (magnification, x4; Thermo Fisher Scientific, Inc.). The colonies were then photographed using HP DeskJet 2132 (Hewlett-Packard Development Company, L.P.).

Wound healing assay. A wound healing assay was performed to analyze cell migration. Briefly, U251MG cells ($1.0x10^5$) were seeded into six-well plates and cultured to 100% confluence. Subsequently, the complete DMEM medium was replaced with serum-free DMEM medium and incubated for 6 h at 37˚C. The confluent cell monolayer was then scratched with a sterile 100-μl pipette tip and treated with 0, 5, 10 or 15 μM MCL. The wounds were visualized at 0 h and after incubation with MCL for 48 h at 37˚C using a Leica DM 14000B light microscope (magnification, x200).

Transwell invasion assay. The upper surface of Transwell plates were precoated with Matrigel and incubated for 30 min at 37˚C for gelation. Briefly, $5x10^4$ U251MG cells/well were plated into the upper chambers of Transwell plates in 400 μl serum-free medium and the lower chambers were filled with 600 μl DMEM supplemented with 10% FBS; both the upper and lower chambers contained 0, 5, 10 or 15 μM MCL. Following 24 h of incubation at 37˚C, the inside surface of the upper membranes was wiped with cotton swabs to remove non-invasive cells. The invasive cells in the lower chamber were fixed with methanol (100%) at room temperature for 10 min and stained with 0.1% crystal violet at room temperature for 30 min. Stained cells were visualized using a Leica DM 14000B light microscope (magnification, x200) in five randomly selected fields of view.

Confocal immunofluorescence imaging (IFI) analysis. The IFI analysis was performed as previously described (9). Briefly, U251MG cells ($1x10^5$ cells/well) were seeded onto coverslips in 6-well plates and treated with 0, 5, 10 or 15 μM MCL for 48 h at 37˚C. Subsequently, the cells were stained with MitoTracker™ Red CMXRos (cat. no. M7512; Invitrogen;

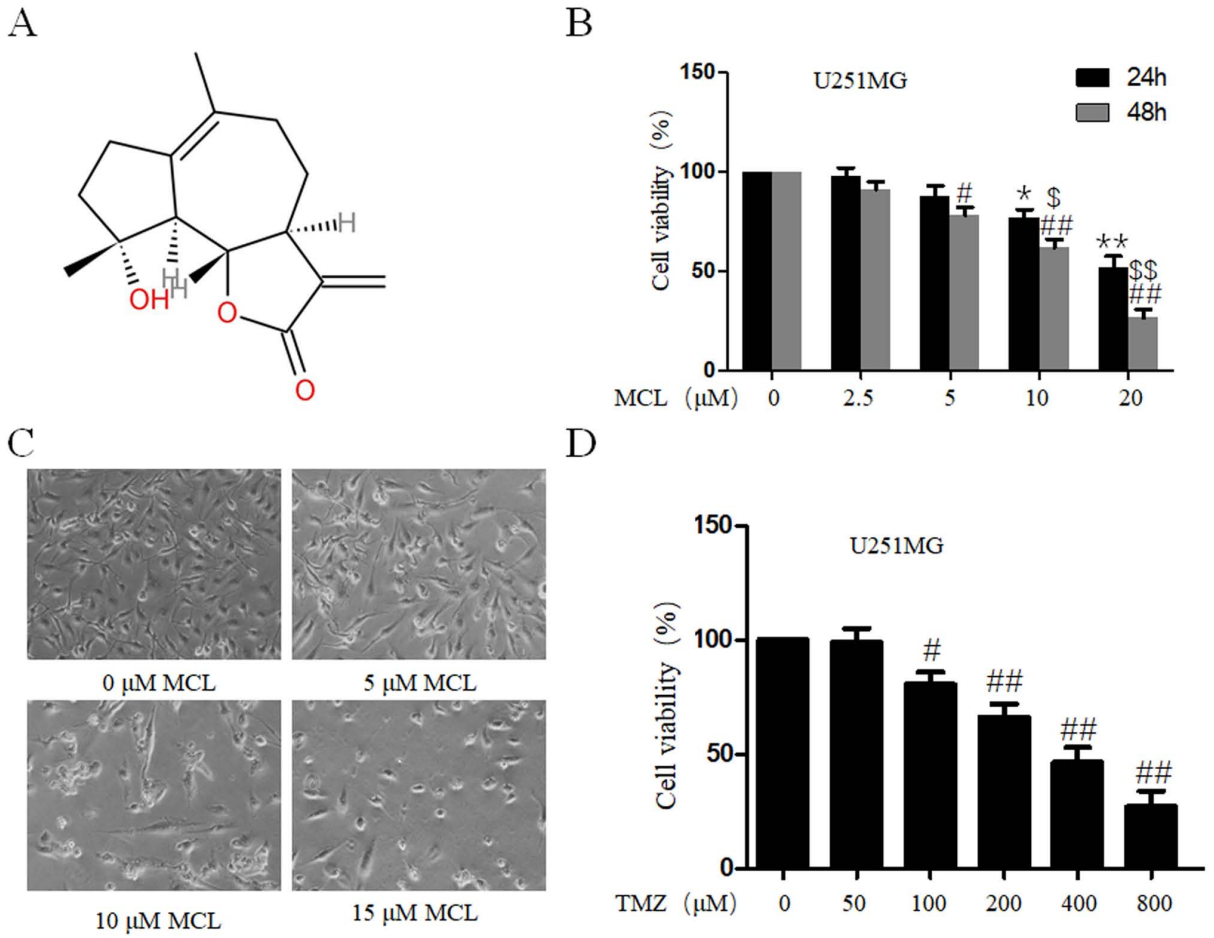

Figure 1. Effects of MCL on cell viability and morphology. (A) Chemical structure of MCL. (B) U251MG cells were treated with MCL at the indicated doses (0, 2.5, 5, 10 or 20 μM). Following treatment for 24 and 48 h, cell viability was determined using a Cell Counting Kit-8 assay. Cells treated with vehicle control (DMSO) were used as the reference group (viability set at 100%). (C) Changes in cell morphology of U251MG cells treated with MCL (0, 5, 10 and 15 μM) were observed. Cells were photographed using a microscope fitted with a digital camera (magnification, x100). (D) U251MG cells were treated with TMZ at the indicated doses (0, 50, 100, 200, 400 or 800 μM). Following treatment for 48 h, cell viability was determined using the Cell Counting Kit-8 assay. Cells treated with vehicle control (DMSO) were used as the reference group (viability set at 100%). Data are presented as the mean ± standard deviation of three times independent experiments. *P<0.05 and **P<0.01 vs. control group at 24h; $^{\#}$P<0.05 and $^{\#\#}$P<0.01 vs. control group at 48 h; $^{\$}$P<0.05 and $^{\$\$}$P<0.01 vs. 24 h group. MCL, micheliolide; TMZ, Temozolomide; DMSO, dimethyl sulfoxide.

Thermo Fisher Scientific, Inc.) for 30 min at 37˚C. Cells were then incubated with an anti-cytochrome *c* primary antibody (1:200) at 4˚C overnight. Following the primary antibody incubation, the cells were incubated with an anti-mouse IgG Alexa Fluor 488-conjugated secondary antibody (1:1,000; cat. no. 4408; Cell Signaling Technology, Inc.) for 1 h in the dark at room temperature. The nuclei were counterstained with DAPI for 5 min in the dark at room temperature and fluorescent slides were visualized using a Leica DM 14000B confocal microscope (magnification, x630).

Western blotting. U251MG cells ($1x10^5$) were treated with MCL (0, 5, 10 and 15 μM) for 48 h at 37˚C, and then total protein was extracted by RIPA lysis buffer and quantified using a bicinchoninic acid assay (Beyotime Institute of Biotechnology). Protein (30-50 μg) was separated via 10-12% SDS-PAGE. The separated proteins were subsequently transferred onto a PVDF membrane and blocked with 5% non-fat dry milk (Beyotime Institute of Biotechnology) for 1h at room temperature. The membranes were then incubated at 4˚C overnight with the following primary antibodies: Anti-cleaved caspase-3 (1:1,000), anti-cleaved caspase-9 (1:1,000), anti-COX-2 (1:1,000), anti-p-IκBα (1:500), anti-IκBα (1:1,000), anti-β-actin (1:2,000), anti-Bcl-2 (1:2,000), anti-Bax (1:2,000), anti-Vimentin (1:1,500), anti-MMP-9 (1:800) and anti-N-cadherin (1:500). Membranes were washed three times with 1X Tris-buffered saline with 0.1% Tween (Beyotime Institute of Biotechnology) and incubated with the anti-rabbit IgG (1:5,000; cat. no. 7074; Cell Signaling Technology, Inc.) or anti-mouse IgG (1:5,000; cat. no. 7076; Cell Signaling Technology, Inc.) secondary antibodies for 2 h at room temperature. Protein bands were visualized using an enhanced chemiluminescence reagent (Beyotime Institute of Biotechnology) and semi-quantification was performed using ImageQuant TL 7.0 software (GE Healthcare).

Reverse transcription (RT-PCR). Total RNA was extracted from U251MG cells ($1x10^5$), which were treated with MCL (0, 5, 10 and 15 μM) for 48 h at 37˚C, using TRIzol® reagent (Invitrogen; Thermo Fisher Scientific, Inc.), according to the manufacturer's protocol. The RNA concentration was determined using a NanoDrop spectrophotometer (Thermo Fisher

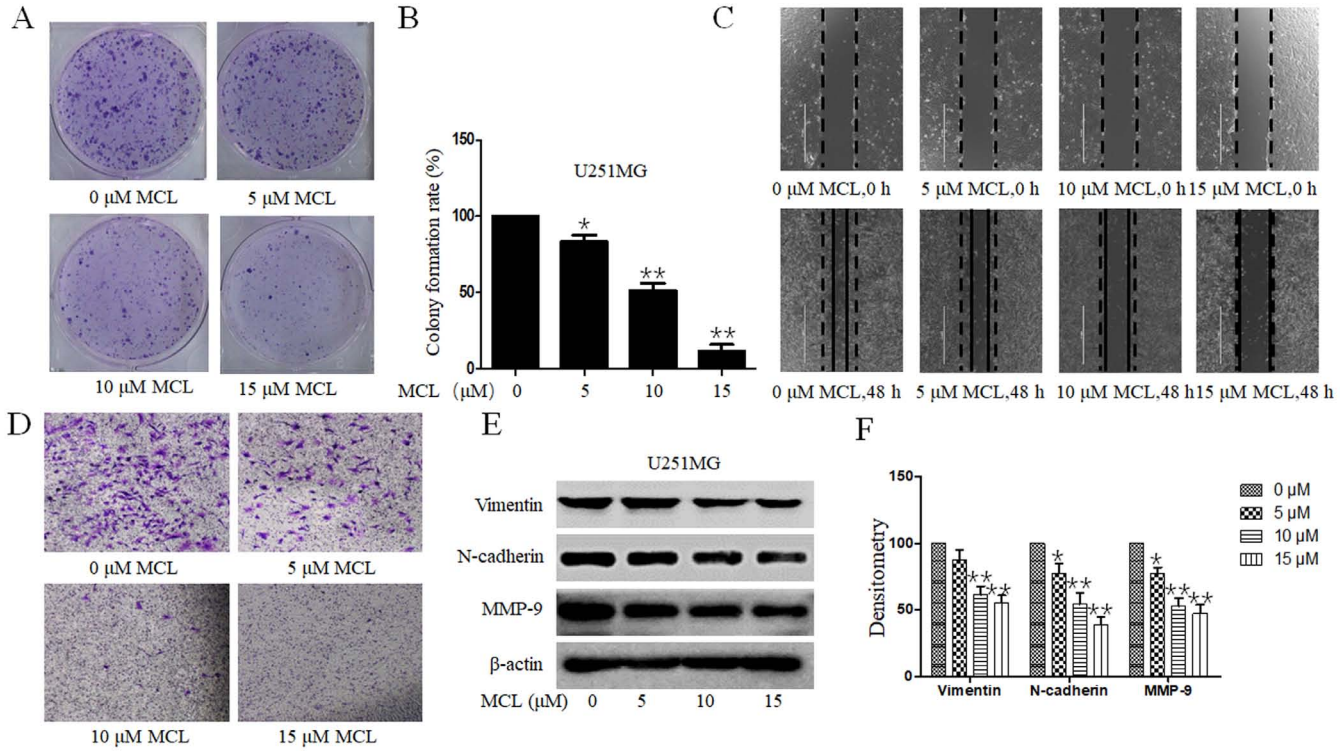

Figure 2. Effects of MCL on colony formation, cell migration and invasion. (A) U251MG cells were treated with MCL (0, 5, 10 or 15 μM) for 24 h. Following culture for 2 weeks, the colony formation of cells was (A) imaged using HP DeskJet 2132 (magnification, 1X) and the (B) colony formation rate was calculated. (C) Effects of MCL on cell migration were analyzed using a wound healing assay. Following 48 h of treatment with MCL (0, 5, 10 or 15 μM), the wound gap was visualized under a microscope. Black dotted line and solid line represent the wound edge of 0 and 48 h, respectively. White solid line represents the scale bars (1,000 μm). (D) Effects of MCL on cell invasion were analyzed using a Transwell Matrigel assay. Following treatment for 24 h, the invasive cells were visualized using a microscope (magnification, x200). (E) Expression levels of levels of MMP-9, N-cadherin and Vimentin were analyzed using western blotting. (F) Quantitative analysis of proteins. Data are presented as the mean ± standard deviation of three times independent experiments. *P<0.05 and **P<0.01 vs. 0 μM MCL, micheliolide; MMP-9, matrix metalloproteinase 9.

Scientific, Inc.) and total RNA was reverse transcribed into cDNA using the PrimeScript RT Reagent kit (cat. no. RR037A; Takara Bio, Inc.), according to the manufacturer's protocol. The following primer pairs were used for the PCR: COX-2 forward, 5'-TCACAGGCTTCCATTGACCAG-3' and reverse, 5'-CCGAGGCTTTTCTACCAGA-3'; and GAPDH forward, 5'-TCTTCGCTTTGTCCTTCGT-3' and reverse, 5'-TGC TGTAGCCAAATTCGTTG-3'. The conditions of the PCR were as follows: 94˚C for 2 min, 35 cycles at 98˚C for 10 sec, 60˚C for 30 sec and 68˚C for 15 sec, and 68˚C for 5 min. Amplification products were analyzed using 1.5% agarose gel electrophoresis stained with GoldenView™ (Dalian Meilun Biology Technology Co., Ltd.) and photographed under ultraviolet light. ImageJ software (National Institutes of Health, version 1.8.0) was used to verify the band intensities as a result of semi-quantitative RT-PCR (30).

Flow cytometric analysis of apoptosis. Flow cytometric analysis was performed to analyze the percentage of sum of early and late apoptotic U251MG cells. Briefly, U251MG cells ($1x10^5$), which were treated with MCL (0, 5, 10 and 15 μM) for 48 h at 37˚C, were stained with Annexin V-FITC and propidium iodide using the Annexin V-FITC Apoptosis Detection kit (cat. no. C1062S; Beyotime Institute of Biotechnology) for 15 min at room temperature, according to the manufacturer's protocol. Apoptotic cells were subsequently analyzed by a BD Accuri™ C6 flow cytometer (BD Biosciences) using the software program BD Accuri™ C6 Plus (version 1.0.227.4).

Statistical analysis. SPSS 17.0 software (SPSS, Inc.) was used for statistical analysis. All data are presented as the mean ± standard deviation and each experiment was performed at least three times. Statistical significances between different groups were determined using a one-way ANOVA, followed by a Tukey's post hoc test for multiple comparisons, and paired Student's t-test for two groups. P<0.05 was considered to indicate a statistically significant difference.

Results

MCL inhibits viability and alters cell morphology in human glioma cells and TMZ inhibits viability in human glioma cells. To investigate the tumor suppressive effect of MCL, (3aS)-3a β,4,5,7,8,9,9aβ,9bα-Octahydro-9β-hydroxy-6,9-dimethyl-3-m ethyleneazuleno[4,5-b]furan-2(3H)-one (Fig. 1A), the effects of MCL on cell viability in human glioma U251MG cells were determined using a CCK-8 assay. MCL inhibited the cell viability of U251MG cells in both a time- and dose-dependent manner (Fig. 1B), and the IC50 for 48 h was 12.586±1.632 μM. In order to further investigate the effects of MCL on cell phenotype, mRNA and protein, we choose 5, 10, 15 μM MCL for the next experiment. The effect of MCL on cell morphology was also investigated in U251MG cells; compared with the

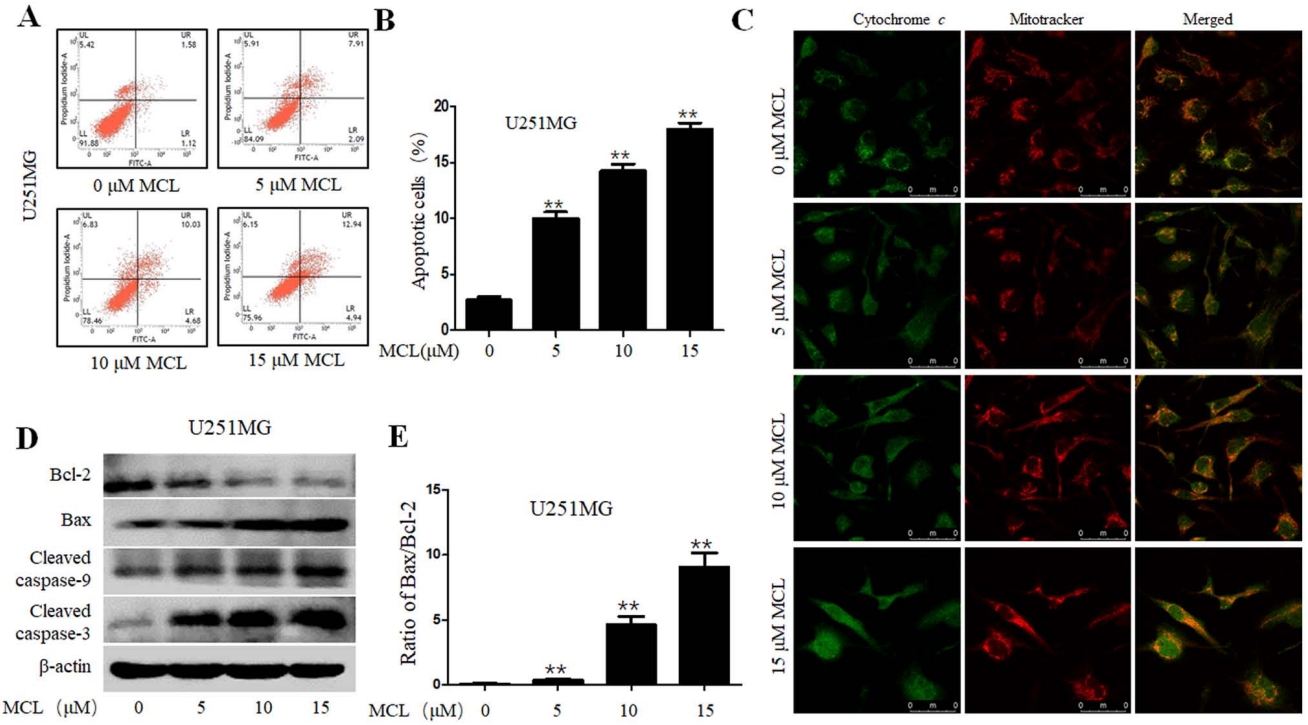

Figure 3. Effects of MCL on caspase-dependent apoptosis. U251MG cells were treated with MCL (0, 5, 10 or 15 μM) for 48 h. (A) Apoptotic levels were determined by flow cytometric analysis and the (B) percentage of sum of early and late apoptotic cells was calculated. (C) Release of cytochrome *c* from the mitochondria to the cytoplasm was observed using immunofluorescence imaging analysis (magnification, x630). (D) Expression levels of cleaved caspase-3, cleaved caspase-9 and Bax/Bcl-2 proteins were analyzed using western blotting. (E) Ratio of Bax/Bcl-2. Data are presented as the mean ± standard deviation of three times independent experiments. **P<0.01 vs. 0 μM MCL. MCL, micheliolide.

0 μM MCL group, MCL treatment (10 and 15 μM) induced cell wrinkles, reduced cytoplasm and reduced the formation of filopodia (Fig. 1C). To investigate the anti-tumor ability of TMZ, the cell viability of human glioma U251MG cells was determined using a CCK-8 assay. As shown in Fig. 1D, cell viability of U251MG cells was reduced in a dose-dependent manner with TMZ treatment, and the IC50 for 48 h was 445.823±59.625 μM. The results indicated that MCL may exhibit marked antitumor effects in human glioma.

MCL inhibits clonogenesis, and the migratory and invasive ability of U251MG cells. The influence of MCL on the clonogenic ability of U251MG cells was evaluated. Consistent with the inhibition over cell viability, MCL treatment significantly inhibited the colony formation ability in a dose-dependent manner compared with the control group (Fig. 2A and B). The inhibitory effects of MCL treatment on tumor cell migration and invasion in U251MG cells were subsequently investigated using wound healing and Transwell Matrigel assays, respectively. The migratory ability of U251MG cells was markedly suppressed in a dose-dependent manner following the treatment of 5, 10 or 15 μM compared with the control group (Fig. 2C). The Transwell Matrigel assay also revealed similar results following MCL treatment (Fig. 2D). Furthermore, to analyze the underlying mechanisms of MCL on cell migration, the relative protein expression levels of MMP-9, N-Cadherin and Vimentin were analyzed. The expression levels of these proteins were downregulated a dose-dependent manner following MCL treatment compared with the control group (Fig. 2E and F). The results suggested that MCL not only inhibited cell viability, but also inhibited cell migration and invasion.

MCL promotes apoptosis through modulating cytochrome c and caspase signaling. Apoptosis induction has been identified as a therapeutic target for all types of cancer treatments (31). Thus, the present study aimed to determine whether the inhibition over cell viability induced by MCL was related to the activation of the apoptotic pathway. The results revealed that MCL significantly induced apoptosis in a dose-dependent manner, from 2.7% in the control group to 17.9% in the 15 μM MCL group (Fig. 3A and B). Previous studies have reported that cytochrome *c* released into the cytoplasm from the mitochondrial intermembrane activated cell apoptosis (32). Thus, IFI analysis was performed to determine whether MCL could promote cytochrome *c* release in U251MG cells, by detecting the co-localization of cytochrome *c* and mitochondria. The IFI results revealed that MCL treatment triggered cytochrome *c* release from the inter-mitochondrial space into the cytosol (Fig. 3C). Furthermore, to determine the mechanisms underlying MCL-induced cell apoptosis, the expression levels of cell apoptosis-related proteins, such as caspase-3, caspase-9, Bax and Bcl-2, were also analyzed using western blotting in U251MG cells. Compared with the control group, MCL treatment upregulated the protein expression levels of cleaved caspase-3 and -9 and Bax, while downregulating Bcl-2 protein expression levels, and the Bax/Bcl-2 ratio was also upregulated in a dose-dependent manner (Fig. 3D and E). These results indicated that MCL may promote cell apoptosis through triggering cytochrome *c* release into the cytoplasm and facilitating the activation of multiple caspase cascades.

MCL downregulates COX-2 expression levels and NF-κB activity. COX-2 is often induced by inflammatory signals

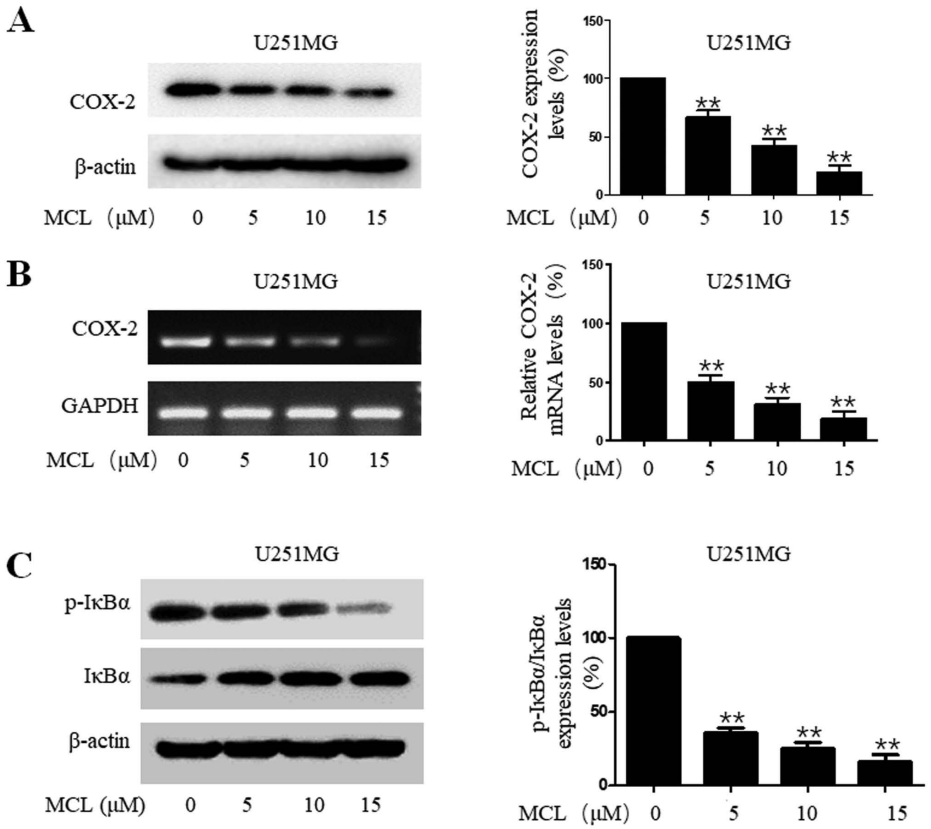

Figure 4. Effects of MCL on NF-κB/COX-2 signaling. U251MG cells were treated with MCL (0, 5, 10 or 15 μM) for 48 h. (A) Protein expression levels of COX-2 were analyzed using western blotting and quantitative analysis of the proteins. (B) mRNA expression levels of COX-2 were analyzed and quantified using reverse transcription-polymerase chain reaction. (C) Expression levels of IκBα and p-IκBα protein were analyzed using western blotting and quantitative analysis of the proteins. Data are presented as the mean ± standard deviation of three times independent experiments. **P<0.01 vs. 0 μM MCL. MCL, micheliolide; COX-2, cyclooxygenase-2; p-, phosphorylated.

and has been identified to promote tumor development (33). Accumulating evidence has indicated that COX-2 expression levels are markedly upregulated in a high percentage of gliomas (33,34). Thus, the effects of MCL on COX-2 expression levels were investigated. MCL treatment significantly downregulated COX-2 expression levels at both the protein and mRNA level in a dose-dependent manner in U251MG cells compared with the control group (Fig. 4A and B). Since COX-2 expression levels were discovered to be tightly controlled by the transcription factor NF-κB in numerous types of cancer (35,36), the effect of MCL on NF-κB activity was also investigated, through determining the degradation of IκBα, an essential event for the activation of NF-κB signaling (37), which occurs through its phosphorylation. The results demonstrated that MCL treatment significantly downregulated the ratio of p-IκBα/IκBα protein expression levels compared with the control group. Meanwhile, on an individual basis, MCL treatment downregulated the expression levels of p-IκBα, while upregulating the expression levels of IκBα (Fig. 4C). Based on these results, it was suggested that MCL may suppress the degradation of IκBα and inhibit the activation of the NF-κB signaling pathway.

Overall, these findings supported the hypothesis that MCL may exhibit a strong inhibitory effect on NF-κB/COX-2 signaling and suppress the proliferation of human glioma carcinoma.

Discussion

In the past few years, Chinese medical herbs have received increasing attention due to their long history of clinical application, low toxicity and therapeutic potential in various types of disease, including numerous types of cancer, such as lung cancer, breast cancer and glioma (9,17,21). MCL is an extract isolated from *Michelia compressa* and *Michelia champaca*, which has been discovered to possess various physiological and pharmacological properties, such as anti-inflammatory and anticancer activities via various signaling pathways, such as PI3K/Akt, NF-kB and MAPK signaling (22-26). However, to the best of our knowledge, its detailed mechanisms of action have not been fully elucidated.

The results of the present study revealed that MCL exerted antitumor effects in human glioma. Previous research has reported that MCL exhibited significant anticancer effects through activating the cytochrome *c*/caspase-dependent apoptotic pathway, thereby downregulating the expression levels of COX-2 by inactivating NF-κB signaling (38,39). To the best of our knowledge, the current study was the first report demonstrating the therapeutic effect of MCL on COX-2 expression levels and its underlying mechanism of action in glioma.

In the present study, MCL inhibited cell viability in human glioma cells at dose of 5, 10 and 15 μM, demonstrating a 48 h half maximal inhibitory concentration (IC_{50}) value of 12.586±1.632 μM; however, although 12.586±1.632 μM MCL

inhibited the survival of tumor cells, to study the antitumor mechanism of MCL, only survival cells were collected and used in western blotting and RT-PCR experiments. Thus, the present study used MCL at concentrations of 5, 10 or 15 μM, and these concentrations did not affect the results. The results of the present study suggested that MCL may inhibit the migration and invasion of U251MG cells through downregulating the expression levels of N-cadherin, Vimentin and MMP-9. To observe the effects of MCL treatment on cell morphology, the cell density was required to be low; however, for the wound healing assay, U251MG cells were cultured to 100% confluence as a high cell density was required. This provides reasoning for why the cell morphology was different for these two assays following the treatment with 15 μM MCL.

Inflammation is involved in multiple different stages of tumor development, including the initiation, promotion and migration (40,41). In previous studies, the expression levels of COX-2 were reported to be significantly overexpressed in patients with glioma, positively correlated with glioma malignancy and negatively correlated with prognosis (19,20). In the current study, MCL significantly downregulated COX-2 expression levels, alongside inhibiting U251MG cell viability and migration, while inducing cell apoptosis. COX-2 expression levels are strictly transcriptionally controlled by several regulatory elements, including NF-κB, which serves important roles in COX-2 promoter activity (42). However, in the canonical pathway, inactive NF-κB residues are sequestered in the cytoplasm through association with inhibitory proteins such as IκB (37). IκB degradation is a crucial step for NF-κB activation; IkBs are rapidly phosphorylated by the active IκB kinase complex and further ubiquitinated by the proteasome (43). Consequently, activated NF-κB proteins (p50/p65 heterodimers) translocate from the cytoplasm to the nucleus, where they bind to the promoters of target genes and regulate their expression, such as COX-2 (9). Thus, inhibiting NF-κB activation may be a beneficial treatment strategy for human gliomas. In the present study, the results demonstrated that MCL treatment inhibited the phosphorylation of IκBα, suggesting attenuation of the NF-κB signaling pathway, thereby downregulating COX-2 expression levels, as observed.

Over the past decade, temozolomide (TMZ) has been commonly used as an effective imidazotetrazine agent against glioma (44,45). The present study investigated the inhibitory effects of TMZ on cell proliferation in human glioma U251MG cells; following 48 h, the IC_{50} value of TMZ was 445.823 μM, while the IC_{50} value of MCL in the present study was 12.586 μM. Furthermore, the antitumor activity was increased ~35-fold following MCL treatment. These findings indicated that MCL may be an effective and alternative antitumor agent for the treatment of human glioma carcinomas.

In conclusion, the results of the present study revealed the potential of MCL to effectively inhibit the biological properties of human gliomas in a number of ways, that is inhibition of invasion/migration and the NF-κB signaling pathway. In addition, the results discovered that the anticancer properties of MCL may be mediated, at least in part, via inhibition of the NF-κB/COX-2 signaling pathway. Thus, the present findings provided preclinical evidence for the development of MCL as a potential agent for the treatment of human glioma carcinomas.

Acknowledgements

Not applicable.

Funding

The present study was supported by the Health Commission of Hubei Province Science Research Project (grant nos. WJ2019H544 and WJ2019H557) and Three Gorges University Hubei Key Laboratory of Tumor Microenvironment and Immunotherapy (grant no. 2019KZL07).

Availability of data and materials

All data generated or analyzed during this study are included in this published article.

Authors' contributions

JZ and FS conceived and designed the experiments. DF, ML, YL, XJZ, HS and XZ performed the experiments. DF, ML and YL conducted the statistical analysis. DF, ML and XJZ drafted the initial manuscript. All authors have read and approved the final manuscript.

Ethics approval and consent to participate

Not applicable.

Patient consent for publication

Not applicable.

Competing interests

The authors declare that they have no competing interests.

References

1. McNeill KA: Epidemiology of brain tumors. Neurol Clin 34: 981-998, 2016.
2. Hu J, Cao X, Pang D, Luo Q, Zou Y, Feng B, Li L, Chen Z and Huang C: Tumor grade related expression of neuroglobin is negatively regulated by PPARgamma and confers antioxidant activity in glioma progression. Redox Biol 12: 682-689, 2017.
3. Sabo B: Primary malignant brain tumours, psychosocial distress and the intimate partner experience: What do we know? Can J Neurosci Nurs 36: 9-15, 2014.
4. Vannini E, Maltese F, Olimpico F, Fabbri A, Costa M, Caleo M and Baroncelli L: Progression of motor deficits in glioma-bearing mice: Impact of CNF1 therapy at symptomatic stages. Oncotarget 8: 23539-23550, 2017.
5. Chi G, Xu D, Zhang B and Yang F: Matrine induces apoptosis and autophagy of glioma cell line U251 by regulation of circRNA-104075/BCL-9. Chem Biol Interact 308: 198-205, 2019.
6. Krex D, Klink B, Hartmann C, von Deimling A, Pietsch T, Simon M, Sabel M, Steinbach JP, Heese O, Reifenberger G, *et al*: Long-term survival with glioblastoma multiforme. Brain 130: 2596-2606, 2007.
7. Tso JL, Yang S, Menjivar JC, Yamada K, Zhang Y, Hong I, Bui Y, Stream A, McBride WH, Liau LM, *et al*: Bone morphogenetic protein 7 sensitizes O6-methylguanine methyltransferase expressing-glioblastoma stem cells to clinically relevant dose of temozolomide. Mol Cancer 14: 189, 2015.
8. MacDonald N: Chronic inflammatory states: Their relationship to cancer prognosis and symptoms. J R Coll Physicians Edinb 41: 246-253, 2011.

9. Zhu J, Zhao J, Yu Z, Shrestha S, Song J, Liu W, Lan W, Xing J, Liu S, Chen C, *et al*: Epoxymicheliolide, a novelguaiane-type sesquiterpene lactone, inhibits NF-κB/COX-2 signaling pathways by targeting leucine 281 and leucine 25 in IKKβ in renal cell carcinoma. Int J Oncol 53: 987-1000, 2018.
10. Murata M: Inflammation and cancer. Environ Health Prev Med 23: 50, 2018.
11. Liu Q, Li G, Li R, Shen J, He Q, Deng L, Zhang C and Zhang J: IL-6 promotion of glioblastoma cell invasion and angiogenesis in U251 and T98G cell lines. J Neurooncol 100: 165-176, 2010.
12. Madan E, Dikshit B, Gowda SH, Srivastava C, Sarkar C, Chattopadhyay P, Sinha S and Chosdol K: FAT1 is a novel upstream regulator of HIF1alpha and invasion of high grade glioma. Int J Cancer 139: 2570-2582, 2016.
13. Lindholm J: A century of pituitary surgery: Schloffer's legacy. Neurosurgery 61: 865-868, 2007.
14. Schwitalla S, Ziegler PK, Horst D, Becker V, Kerle I, Begus-Nahrmann Y, Lechel A, Rudolph KL, Langer R, Slotta-Huspenina J, *et al*: Loss of p53 in enterocytes generates an inflammatory microenvironment enabling invasion and lymph node metastasis of carcinogen-induced colorectal tumors. Cancer Cell 23: 93-106, 2013.
15. Grivennikov SI, Greten FR and Karin M: Immunity, inflammation, and cancer. Cell 140: 883-899, 2010.
16. Wang X, Yu Z, Wang C, Cheng W, Tian X, Huo X, Wang Y, Sun C, Feng L, Xing J, *et al*: Alantolactone, a natural sesquiterpene lactone, has potent antitumor activity against glioblastoma by targeting IKKbeta kinase activity and interrupting NF-κB/COX-2-mediated signaling cascades. J Exp Clin Cancer Res 36: 93, 2017.
17. Peng Y, Wang Y, Tang N, Sun D, Lan Y, Yu Z, Zhao X, Feng L, Zhang B, Jin L, *et al*: Andrographolide inhibits breast cancer through suppressing COX-2 expression and angiogenesis via inactivation of p300 signaling and VEGF pathway. J Exp Clin Cancer Res 37: 248, 2018.
18. Perdiki M, Korkolopoulou P, Thymara I, Agrogiannis G, Piperi C, Boviatsis E, Kotsiakis X, Angelidakis D, Diamantopoulou K, Thomas-Tsagli E and Patsouris E: Cyclooxygenase-2 expression in astrocytomas. Relationship with microvascular parameters, angiogenic factors expression and survival. Mol Cell Biochem 295: 75-83, 2006.
19. Festa-Vasconcellos JS, Piranda DN, Amaral LM, Indio-do-Brasil V, Koifman S and Vianna-Jorge R: Polymorphisms in cycloxygenase-2 gene and breast cancer prognosis: Association between PTGS2 haplotypes and histopathological features. Breast Cancer Res Treat 132: 251-258, 2011.
20. Chen G, Li X, Yang J, Li J, Wang X, He J and Huang Z: Prognostic significance of cyclooxygenase-2 expression in patients with hepatocellular carcinoma: A meta-analysis. Arch Med Sci 5: 1110-1117, 2016.
21. Liu X, Zhao P, Wang X, Wang L, Zhu Y, Song Y and Gao W: Celastrol mediates autophagy and apoptosis via the ROS/JNK and Akt/mTOR signaling pathways in glioma cells. J Exp Clin Cancer Res 38: 184, 2019.
22. Viennois E, Xiao B, Ayyadurai S, Wang L, Wang PG, Zhang Q, Chen Y and Merlin D: Micheliolide, a new sesquiterpene lactone that inhibits intestinal inflammation and colitis-associated cancer. Lab Invest 94: 950-965, 2014.
23. Qin X, Jiang X, Jiang X, Wang Y, Miao Z, He W, Yang G, Lv Z, Yu Y and Zheng Y: Micheliolide inhibits LPS-induced inflammatory response and protects mice from LPS challenge. Sci Rep 6: 23240, 2016.
24. Kalantary-Charvadeh A, Sanajou D, Hemmati-Dinarvand M, Marandi Y, Khojastehfard M, Hajipour H, Mesgari-Abbasi M, Roshangar L and Nazari Soltan Ahmad S: Micheliolide protects against doxorubicin-induced cardiotoxicity in mice by regulating PI3K/Akt/NF-kB signaling pathway. Cardiovasc Toxicol 19: 297-305, 2019.
25. Li J, Li S, Guo J, Li Q, Long J, Ma C, Ding Y, Yan C, Li L, Wu Z, *et al*: Natural product micheliolide (MCL) irreversibly activates pyruvate kinase M2 and suppresses leukemia. J Med Chem 61: 4155-4164, 2018.
26. Peng F, Li H, Li S, Wang Y, Liu W, Gong W, Yin B, Chen S, Zhang Y, Luo C, *et al*: Micheliolide ameliorates renal fibrosis by suppressing the Mtdh/BMP/MAPK pathway. Lab Invest 99: 1092-1106, 2019.
27. Xi XN, Liu N, Wang QQ, Wu HT, He HB, Wang LL, Zhang TJ, Sun L, Yin Z, Chen Y and Lu YX: Pharmacokinetics, tissue distribution and excretion of ACT001 in Sprague-Dawley rats and metabolism of ACT001. J Chromatogr B Analyt Technol Biomed Life Sci 1104: 29-39, 2019.
28. Zhang Q, Lu Y, Ding Y, Zhai J, Ji Q, Ma W, Yang M, Fan H, Long J, Tong Z, *et al*: Guaianolide sesquiterpene lactones, a source to discover agents that selectively inhibit acute myelogenous leukemia stem and progenitor cells. J Med Chem 55: 8757-8769, 2012.
29. Wang Y, Zhang J, Yang Y, Liu Q, Xu G, Zhang R and Pang Q: ROS generation and autophagosome accumulation contribute to the DMAMCL-induced inhibition of glioma cell proliferation by regulating the ROS/MAPK signaling pathway and suppressing the Akt/mTOR signaling pathway. Onco Targets Ther 12: 1867-1880, 2019.
30. Nanes BA: Slide Set: Reproducible image analysis and batch processing with ImageJ. BioTechniques 59: 269-278, 2015.
31. Wu S, Luo C, Li F, Hameed NUF, Jin Q and Zhang J: Silencing expression of PHF14 in glioblastoma promotes apoptosis, mitigates proliferation and invasiveness via Wnt signal pathway. Cancer Cell Int 19: 314, 2019.
32. Amin RM, Elfeky SA, Verwanger T and Krammer B: Fluorescence-based CdTe nanosensor for sensitive detection of cytochrome C. Biosens Bioelectron 98: 415-420, 2017.
33. Zhang F, Chu J and Wang F: Expression and clinical significance of cyclooxygenase 2 and survivin in human gliomas. Oncol Lett 14: 1303-1308, 2017.
34. Xu K, Wang L and Shu HK: COX-2 overexpression increases malignant potential of human glioma cells through Id1. Oncotarget 5: 1241-1252, 2014.
35. Annabi B, Laflamme C, Sina A, Lachambre MP and Beliveau R: A MT1-MMP/NF-kappaB signaling axis as a checkpoint controller of COX-2 expression in CD133+U87 glioblastoma cells. J Neuroinflammation 6: 8, 2009.
36. Ye Y, Shan Y, Bao C, Hu Y and Wang L: Ginsenoside Rg1 protects against hind-limb ischemia reperfusion induced lung injury via NF-κB/COX-2 signaling pathway. Int Immunopharmacol 60: 96-103, 2018.
37. Karin M and Ben-Neriah Y: Phosphorylation meets ubiquitination: The control of NF-[kappa]B activity. Annu Rev Immunol 18: 621-663, 2000.
38. Zhong J, Gong W, Chen J, Qing Y, Wu S, Li H, Huang C, Chen Y, Wang Y, Xu Z, *et al*: Micheliolide alleviates hepatic steatosis in db/db mice by inhibiting inflammation and promoting autophagy via PPAR-γ-mediated NF-κB and AMPK/mTOR signaling. Int Immunopharmacol 59: 197-208, 2018.
39. Jia Y, Zhou L, Tian C, Shi Y, Wang C and Tong Z: Dynamin-related protein 1 is involved in micheliolide-induced breast cancer cell death. Onco Targets Ther 8: 3371-3381, 2015.
40. Tao Y, Yuan D, Pang H, Wu H, Liu D, Jin N, Wu N, Qiu J and Cao Y: Dynamic impact of in fl ammation-based indices in colorectal cancer patients receiving FOLFOX-based chemotherapy. Cancer Manag Res 11: 2817-2829, 2019.
41. Jiang XP, Zhang DX, Teng M, Zhang Q, Zhang JP and Huang YS: Downregulation of CD9 in keratinocyte contributes to cell migration via upregulation of matrix metalloproteinase-9. PLoS One 8: e77806, 2013.
42. Zandi E, Rothwarf DM, Delhase M, Hayakawa M and Karin M: The IkappaB kinase complex (IKK) contains two kinase subunits, IKKalpha and IKKbeta, necessary for IkappaB phosphorylation and NF-kappaB activation. Cell 91: 243-252, 1997.
43. Dong T, Li C, Wang X, Dian L, Zhang X, Li L, Chen S, Cao R, Li L, Huang N, *et al*: Ainsliadimer A selectively inhibits IKKα/β by covalently binding a conserved cysteine. Nat Commun 6: 6522, 2015.
44. Chang L, Su J, Jia X and Ren H: Treating malignant glioma in Chinese patients: Update on temozolomide. Onco Targets Ther 7: 235-244, 2014.
45. Daniel P, Sabri S, Chaddad A, Meehan B, Jean-Claude B, Rak J and Abdulkarim BS: Temozolomide induced hypermutation in glioma: Evolutionary mechanisms and therapeutic opportunities. Front Oncol 9: 41, 2019.